SKI Report 01:45

Research

Composition of Whiskers Grown on Copper in Repository Environment

Hans-Peter Hermansson
Peeter Tarkpea
Stellan Holgersson

November 2001

ISSN 1104-1374
ISRN SKI-R–01/45–SE

SKI Perspective

Background

In the planned repository for spent nuclear fuel in Sweden, according to the KBS-3 concept, a canister consisting of an outer copper shell and an cast iron insert plays an important role to isolate the waste. The function of the copper shell is to give corrosion resistance. SKI has earlier studied different forms of general and localised corrosion on copper, using the results as one basis (among others) in its reviews of SKB's RD&D Programmes and reviews of performance assessments. In theses earlier studies it has been demonstrated that whiskers (dendritic crystals) can grow on copper in an sulphide-containing environment resembling groundwater at repository depths.

Purpose of the project

Corrosion of copper in the form of whisker growth would be more severe to the canister if the corrosion is localised to the root of the whisker rather than affecting a larger area. The purpose of this project is to study the morphology and elemental composition of the whiskers with the aim to get a better understanding of whisker growth and especially if the growth is of local or global character.

Results

A combination of techniques was used for the characterisation of the whiskers and root areas on the copper: Scanning Electron Microscopy with Energy Dispersive Spectrometer (SEM-EDS), X-ray Diffraction (XRD) and Laser Raman Spectroscopy (LRS). The results show that the corrosion layer on copper is stratified with copper oxides, sulphides and possibly carbonates, and that the whiskers show a similar stratification, but in a concentric, cylindrical configuration. There were numerous pits found on the surface, but it was not possible to show that they were root areas of whiskers, partly because the whiskers were fragile and easily fell off.

Continued work

It has not been clearly demonstrated if the whisker growth is a type of localised corrosion, and therefore further experiments are planned. Probably some kind of mechanical support is needed to avoid the whiskers to fall off.

Effects on SKI work

SKI will use the results both in developing its own knowledge of corrosion processes and as a basis in its forthcoming reviews of SKB's programme.

Project information

Responsible for the project at SKI has been Christina Lilja.
SKI reference: 14.9-000317/00181.

SKI Report 01:45

Research

Composition of Whiskers Grown on Copper in Repository Environment

Hans-Peter Hermansson[1 2]
Peeter Tarkpea[1]
Stellan Holgersson[1]

[1]Studsvik Nuclear AB
SE-611 82 Nyköping
Sweden

[2]Luleå University of Technology
SE-971 87 Luleå
Sweden

November 2001

SKI Project Number 00181

Contents

Abstract

There is a hypothesis that a special family of local attack on copper based on growth of whiskers of sulfide, oxide/hydroxide and also carbonate/malachite could appear in the repository environment. It was earlier demonstrated that such whiskers could grow in a laboratory simulated repository environment, containing sulfide. A suggested composition of whiskers has earlier been forwarded but was not demonstrated. In the present work whiskers and their substrates were grown and characterized by investigations with a combination of SEM-EDS, XRD and LRS (Laser Raman Spectroscopy) techniques.

SEM-EDS was used to determine the morphology and an elemental composition and distribution of whiskers and their substrate. A special effort was made to find out if the whisker growth is of a local or global character. The phase status could be determined locally and globally by combining XRD and LRS techniques on whiskers and substrates. Ideally, LRS gives a phase resolution down to a radius of 1 μm on the sample surface. This is of great value as it is of interest to study if there are phase differences in different parts of a whisker. Such information is important to understand the whisker growth mechanism.

Cylindrical samples of pure copper were prepared and exposed to the selected de-aerated model groundwater containing, among other ions, chloride and sulfide. Exposure was performed in sealed glass flasks under de-aerated conditions.

After exposure the copper sample was investigated on the surface, in cross section and on whiskers using the mentioned techniques. The results show that a black, easily detached layer of corrosion products is formed on the sample surface. The corrosion layer was subdivided into at least five parallel strata (probably more) of different composition. Numerous small pits and shallow pitting attacks with a larger radius were observed in the copper metal and the metal surface was in general very rough.

A multitude of very easily detached whiskers or needle-shaped growth forms grew from the surface of the sample throughout the time of exposure. They were very fragile and difficult to prepare for subsequent investigations. A whisker seems to have a core of copper sulfide, which could act as a rapid route of transportation for copper. The concentration of sulfide increases from the root to the top part of the whisker. There are often straight dendritic flanged edges, rich in copper oxide and carbonate, along the sides of the whiskers. The composition is thus very complex. The stratification found in the corrosion layer is also present in a whisker but with a concentric, cylindrical geometry.

When analyzing the corrosion layer, the whiskers had fallen off and because of this no obvious roots or substrate areas for whisker growth were found. It could be speculated if each of the numerous pits observed is situated below a whisker and is part of a whisker substrate or root, but this is not confirmed. To accomplish this, future experiments should be made in an environment that is not limited in sulfide. Furthermore, to prevent the whiskers from detaching, the whiskers should be supported by a porous medium.

Sammanfattning

En hypotes har framlagts att en speciell typ av lokal korrosion på koppar kan uppträda i slutförvarsmiljön. Den bygger på tillväxt av whiskers eller nålformade kristaller som kan tänkas bestå av kopparsulfid, oxid/hydroxid, karbonat/malakit eller en kombination av dessa. Det har redan visats att sådana whiskers kan växa i laboratoriesimulerad förvarsmiljö som innehåller sulfid. En whisker-sammansättning har redan föreslagits, men ej verifierats. I föreliggande arbete har whiskers tagits fram och karakteriserats genom kombinerade undersökningar med SEM-EDS, XRD och LRS (Laser Raman Spektroskopi).

SEM-EDS användes för att klarlägga morfologi och elementsammansättning hos whiskers och deras substrat eller underliggande lager av korrosionsprodukter. En särskild insats ägnades åt att klarlägga om whiskerväxten är av lokal eller global karaktär. Genom att kombinera XRD- och LRS-teknik på whiskers och substrat, kunde fastillstånd bestämmas lokalt och globalt. Under ideala förhållanden ger LRS en radiell upplösning av ca. 1 μm på provytan. Detta är av stort värde eftersom det är av intresse att fastlägga fasskillnader mellan olika delar av en whisker. Sådan information är viktig för att förstå whiskerns tillväxtmekanism.

Cylindrar av koppar exponerades för ett utvalt avluftat modellgrundvatten innehållande bl.a. klorid och sulfid. Exponeringen skedde i slutna glaskärl.

Efter exponeringen undersöktes proven på ytan och i tvärsnitt samt på whiskers med nämnda tekniker. Resultaten visar att det bildas ett svart, mycket lätt avflagnande skikt av korrosionsprodukter på provytan. Skiktet bestod av åtminstone 5 underskikt med olika sammansättning. Kopparmetallen hade generellt en ojämn yta med bl.a. talrika små gropfrätor samt ett antal grunda gropar med stor radie.

Ett stort antal lätt avlossande whiskers växte från ytan vid exponeringen. De var mycket sköra och därför svåra att preparera för de efterföljande undersökningarna. En whisker verkar ha en kärna av kopparsulfid, som möjligen kan fungera som en snabb transportled för kopparjoner. Sulfidkoncentrationen verkar öka mot spetsen. Det finns i allmänhet dendritiska flänsar som löper parallellt med längdaxeln på whiskerns sida. Dendriter och flänsar verkar mest bestå av oxid och karbonat. Whisker-uppbyggnaden är således komplex med en sulfidkärna omgiven av ett yttre oxid/karbonatlager med dendriter. Den skiktning som finns i korrosionsproduktslagret på ytan kan således påvisas även i en whisker, men har där en koncentrisk, cylindrisk geometri.

På grund av att samtliga whiskers hade lossnat från ytorna vid analysen kunde inga uppenbara rot- eller närområden till dessa återfinnas i lagret av korrosionsprodukter. Det kan naturligtvis spekuleras i om de talrika gropfrätnings-angreppen har med whiskerväxten att göra, men detta är ej bekräftat. För att kunna göra det bör framtida experiment utföras i en miljö där tillgänglig sulfid ej är begränsande. Dessutom bör whiskers stödjas av ett poröst medium för att förhindra att de faller bort.

Introduction

Copper will be used for fuel canisters in a Swedish deep underground final repository of spent nuclear fuel, as proposed by the Swedish Nuclear Fuel and Waste Management Co (SKB). In the last ten years, the Swedish Nuclear Power Inspectorate (SKI) has instigated several studies on the corrosion of copper. This is a part of a general improvement of the knowledge basis in this area. The knowledge basis has been reviewed in several literature studies [1-5]. General and localized corrosion have been studied, both experimentally [3-6] and theoretically [5,7-9].

There is a hypothesis that a special family of local attack on copper based on growth of dendritic crystals, so called whiskers, could appear in the repository environment [3,5,8]. The whisker growth is based on the formation of copper sulfide, oxide/hydroxide and also carbonate/malachite phases. It has already been demonstrated that such whiskers can grow on copper in a laboratory simulated, repository-related environment, containing sulfide. A suggested composition of such whiskers has been forwarded [5] but not demonstrated. In the present work whiskers are characterized by investigations with a combination of Scanning Electron Microscopy with Energy Dispersive Spectrometer (SEM-EDS), X-ray Diffraction (XRD) and Laser Raman Spectroscopy (LRS) techniques.

SEM-EDS is used to determine the morphology and elemental composition of whiskers and substrate. A special effort is made to find out if the whisker growth is of a local or global character. The elemental distribution is determined in a whisker, in its substrate and in surrounding corrosion products that are not a direct substrate for a whisker.

The phase status can be determined locally and globally by combining XRD and LRS techniques on whiskers and substrates. Ideally, LRS gives a resolution down to a radius of 1 μm on the sample surface. It can therefore be used to study details in a whisker concerning phase composition and distribution. This is of great value as it is of interest to study if the root part of the whisker differs in composition from the outer parts.

Experimental

Background

Exposures of copper samples of different sizes and geometry in a series of environments of interest to simulate the conditions in the repository have been made before [3-6]. In some of those cases whisker growth was observed. For the present work the cylindrical type of copper sample already used [5] and the chemical environment as accounted in Table 1 was selected.

Copper sample

The sample preparation procedure was similar to what was used in earlier copper corrosion studies [5]. The chosen cylindrical sample (Figure 1) was polished with a 1000 mesh polish paper and ultrasonically cleaned in water, acetone and ethanol. After cleaning the sample it was stored in a desiccator until it was immersed in the chosen model groundwater, the composition of which is found in Table 1.

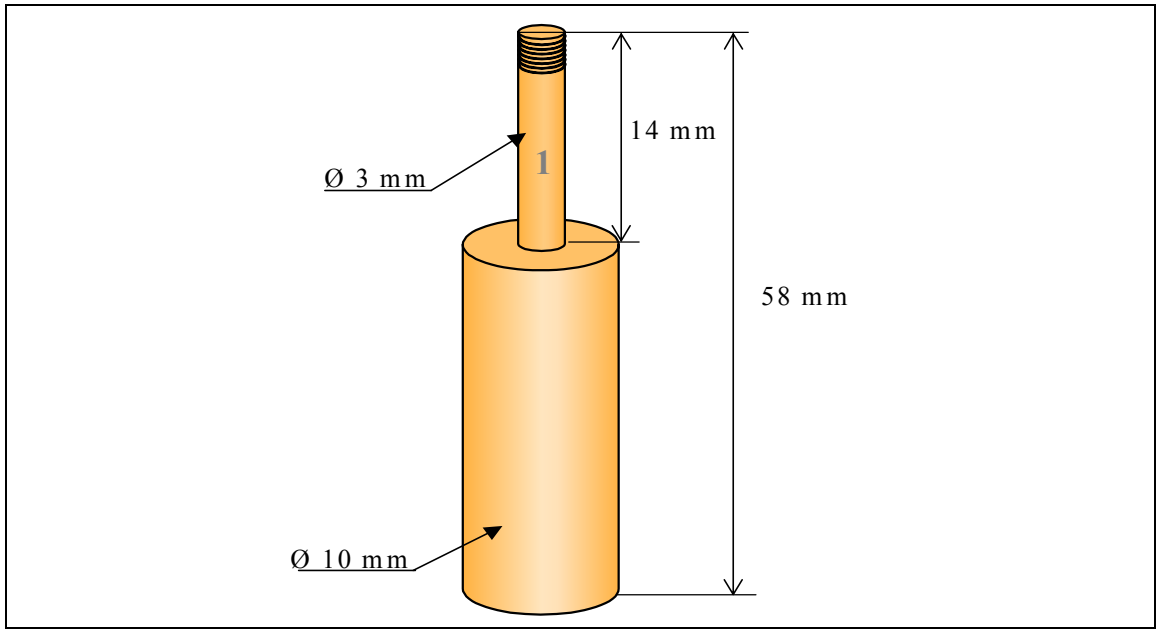

Figure 1
The geometry and size of the cylindrical copper sample.

Table 1
Synthetic groundwater used in the experiment.

SALT/ppm		**CATION** /ppm		**ANION**/ppm	
NaCl	100	Na^+	40	Cl^-	60
$CaCl_2$	30	Ca^+	10.8	Cl^-	19.2
Na_2SO_4	2.5	Na^+	0.8	SO_4^{2-}	1.7
$MgCl_2*6H_2O$	7	Mg^{2+}	0.8	Cl^-	2.4
Na_2S	100	Na^+	59	S^{2-}	41

Whisker growth and examinations

The exposure was carried out at room temperature (20°C) in a glass flask with a volume of 0,5 L. Before immersion of the sample into the solution, most of the dissolved oxygen was removed by bubbling with nitrogen. After immersion of the sample the flask was rapidly sealed off and kept sealed throughout the experiment to minimize the influx of oxygen. However, a small amount of oxygen could be present at the start of the experiment, and diffusion of a very small amount during the experiment cannot be ruled out.

It was found in earlier studies [3-6, 9] that the salt (mainly chloride) concentration of the groundwater is of importance for the formation/non-formation of a protective film on the copper surface. A high enough chloride concentration to simulate a salty ground water environment but low enough to permit a passive film to be formed was therefore selected for the experiments.

It was also found [3,5] that hydrogen sulfide (HS^-) and carbonate (HCO_3^-) ions in the groundwater could be expected to give pitting corrosion on copper under certain conditions. Therefore these species were added to higher concentration in some of the groundwaters studied earlier [3,5]. When synthetic groundwaters with a large range of salts in varying concentrations where compared to waters with only chloride added to the same ionic strength there was no significant difference in the polarization curves of copper [3]. Based on this finding the synthetic groundwaters for the subsequent study [5] where simplified by removing salts present in small amounts in natural groundwater, as long as they where not expected to be of special importance for pitting corrosion on copper. A detailed list of the composition of the groundwaters can be found in the reference [5].

In some of those environments whiskers were observed [5]. A composition of simulated groundwater causing whisker growth was therefore selected for the present experiment, see Table 1.

In the present study whiskers appeared after an exposure time of 2 weeks and the experiment was ended after 2 months when 5-10 mm long whiskers had been grown. Most of the reactions seemed to take place during the first month of the experiment. The

system was carefully drained and whiskers and scaled off flakes of the corrosion product film and the cylinder itself were selected for further investigations by visual inspection, SEM-EDS, XRD and LRS (Laser Raman Spectroscopy).

The surface, detached flakes, as well as a cross section of the sample were investigated in a light optical microscope, in SEM and SEM-EDS. Light optical microscopy was used for a general overview and the selection of parts for SEM and SEM-EDS analyses. Also one of the few whiskers found on the surface was selected and analyzed in SEM-EDS. The SEM-EDS instrument used for this investigation was a JEOL 6300 with a Noran EDS.

The XRD instrument was a Guiner camera for pulverized samples. Standard methods were used for the sample preparation.

The preparation of samples for LRS can be compared with the corresponding for optical microscopy. Laser-raman spectroscopy, LRS is performed with a device resembling an ordinary optical microscope. The sample is placed directly on a x, y, z table, adjusted and exposed to a laser beam. The chemical phases in the sample return Raman radiation that is analyzed in a spectrometer. Analyses were performed with the Renishaw LRS instrument at Luleå University of Technology, LTU.

The instrument at LTU has access to three lasers:

- Argon ion laser (green laser light, 514 nm)
- Helium/Neon laser (red laser light, 632 nm)
- Diode laser (red laser light, 780 nm)

In this case the green argon ion laser was used.

The instrument permits a resolution down to about 1 μm in an optimal case. The penetration depth will vary depending on wavelength and intensity of the laser beam as well as of the optical properties of the sample. The signal from the spectrometer is used by a PC-program to draw Raman spectra as the relative intensity of the scattered Raman radiation as a function of the wave number, cm^{-1}.

The sample can be viewed through the microscope with a video camera. This enables simple handling and positioning of the sample as well as selection of areas of interest for analysis on the surface of the sample. It is also possible to record bitmap pictures of a mediocre quality of the selected sample area.

Results

SEM-EDS of the corrosion layer

A black layer of corrosion products was formed on the sample surface during the exposure. The layer acted as a substrate for whiskers. The layer adhered poorly and therefore flaked off easily from the surface. It detached from several relatively large areas and the flakes sedimented to the bottom of the reaction flask.

The thickness of the corrosion layer was relatively constant around the sample and varied in the range 4 – 6 μm. A picture from optical microscopy of the cross section is shown in Figure 2. In this case the corrosion layer seemed to be composed of up to five parallel separate strata. It can be seen in Figure 2 that the layer splits and that the outer 2 or 3 substrata stick together and scale off. The copper surface under the corrosion layer is very rough and numerous small pits can be observed.

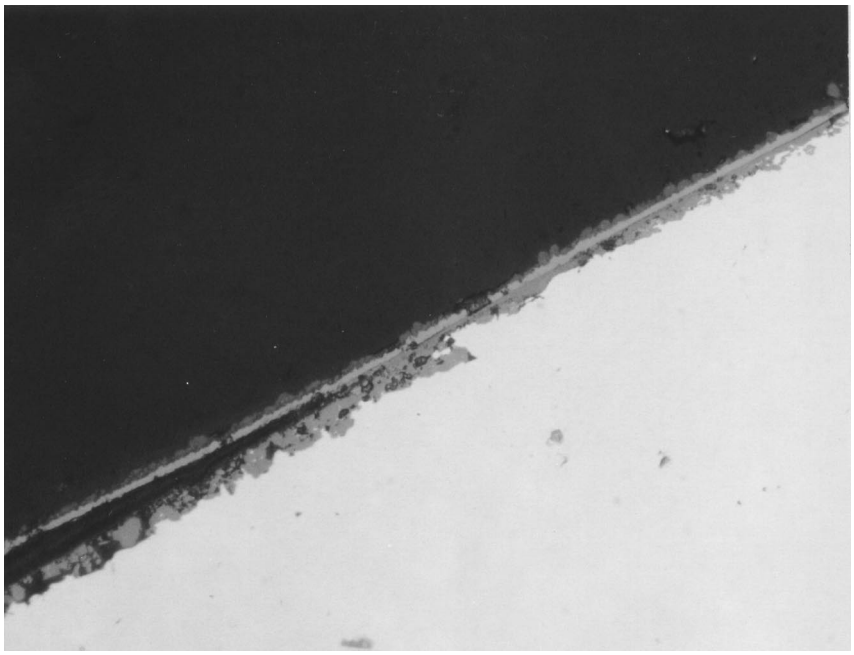

Figure 2
Cross-section of the sample showing scaling-off strata in the corrosion layer. Optical microscopy, X500.

Beside the general roughness with small pits, there were also shallow pitting attacks with a larger radius to be seen in the copper metal. The corrosion layer was up to four times deeper (16 – 25 μm) in the vicinity of such pits compared to the depth outside of pits (4 – 6 μm). An example of a shallow pitting attack is shown in Figure 3. The outer strata of the corrosion layers have scaled off in a way shown in Figure 2 and the layer shown is therefore thinner than it was before sampling.

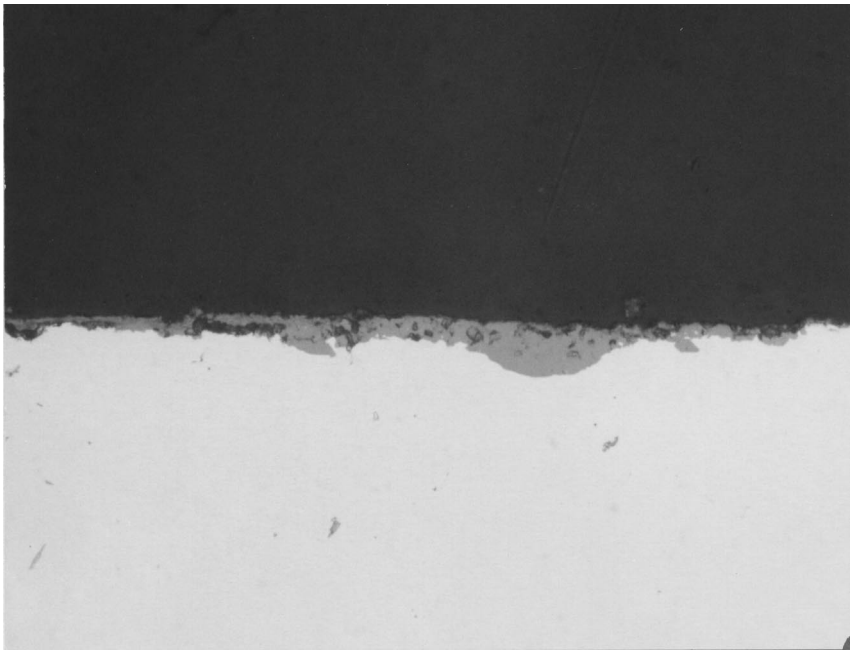

Figure 3
Cross-section of the sample, showing an area with remaining layer strata and a shallow pit. Optical microscopy, X500.

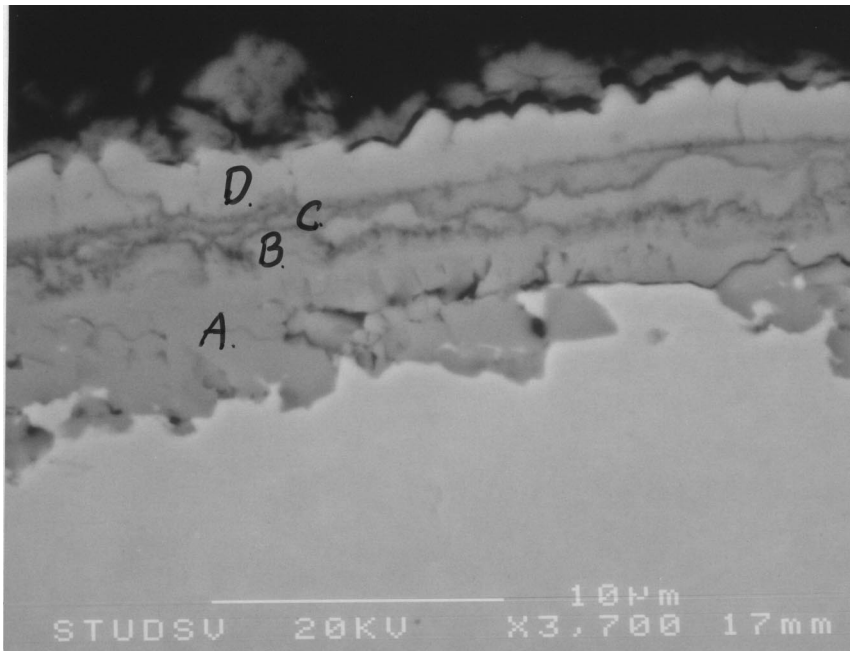

Figure 4
SEM picture of sub-strata of the corrosion product layer.

The typical subdivision of the corrosion layer in sub-strata can be easily seen in SEM-pictures as in Figure 4. The different sub-strata marked A-D in Figure 4 were point analyzed in SEM-EDS. The results are accounted in Appendix A, Figures A1-A4.

The two outer sub-strata C and D contain sulfur in this case. The next sub-stratum B seems to contain a smaller amount of sulfur than the outermost. Those outer layers could consist of copper sulfides. As a speculation it is suggested that there is Cu_2S in the B sub-stratum and CuS in the C and D sub-strata. It should be reminded, however, that there are many possible Cu-S containing phases that are possible as well as more complicated phases. The B sub-stratum is the one that seems to scale off from the next sub-stratum A. See Figures 2 and 4.

The sub-stratum A, under the sulfur rich layers, probably consists of copper oxide. The inner sub-strata also contain small amounts of Cl and Si. However, there is no Si closest to the metal. Au seen in SEM-EDS spectra is, of course, an artifact from sample preparation. Sulfur is not present closest to the metal and it was not present in the innermost sub-stratum A, see Figures A1-A4. The concentration of sulfur thus seems to increase outwards in the layer structure.

As have been pointed out earlier, the outer layers scale off easily and this is probably the case here too. This means that there have probably been one or more strata of sulfide and/or oxide/carbonate present outside the sulfur rich C and D strata marked in Figure 4.

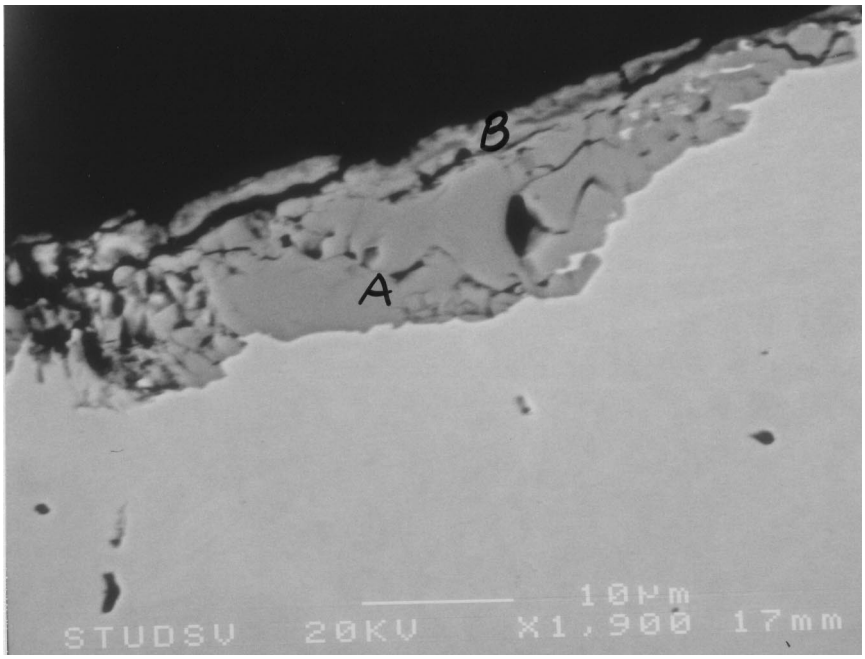

Figure 5
SEM picture of a pitting corrosion attack.

An example of a pit investigated in SEM-EDS is shown in Figure 5. The sulfur rich layer expected in Figure 5 has detached and is not seen in the picture. Sulfur and silicon were found in the pit (A) and also in the evenly thick layer on top of the pit (B). It should be emphasized that there were no traces of chlorine in the pit itself. Sulfur cannot be found closest to the metal but in the outer layers as seen in the point analyses accounted in Appendix A, Figures A5 and A6.

SEM-EDS of flakes

As have been shown, the outer strata of the corrosion layer were easily detached. They formed flakes that either remained on the surface or detached to form a deposit on the bottom of the flask. As such layers were suspected to contain substrate areas or "roots" of whiskers they were collected and specifically investigated to find such areas.

One part of the sample surface from which scaling-off has occurred is shown in Figure 6. Deposited flakes of the detached corrosion layer are shown in Figure 7.

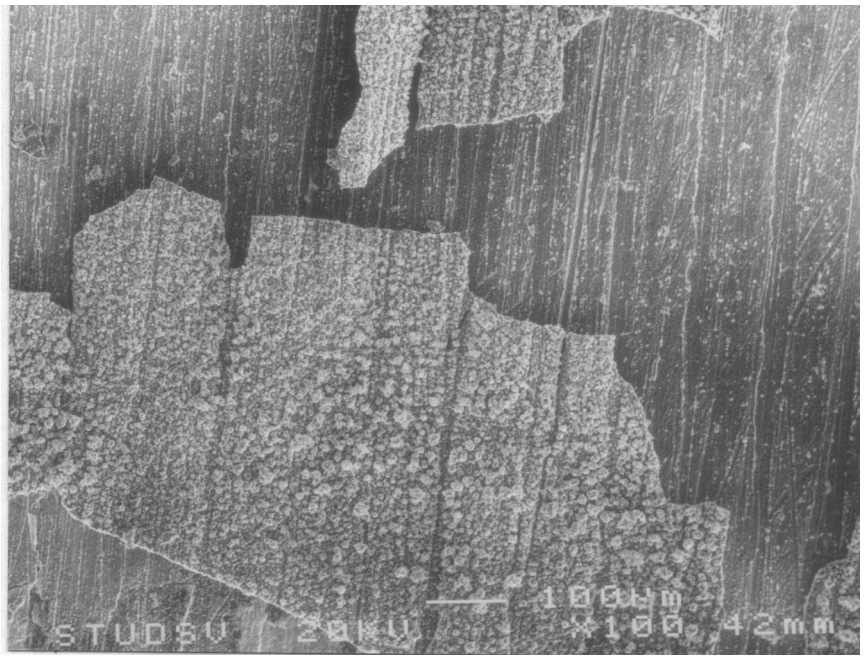

Figure 6
SEM picture of sample surface from which scaling-off has occurred.

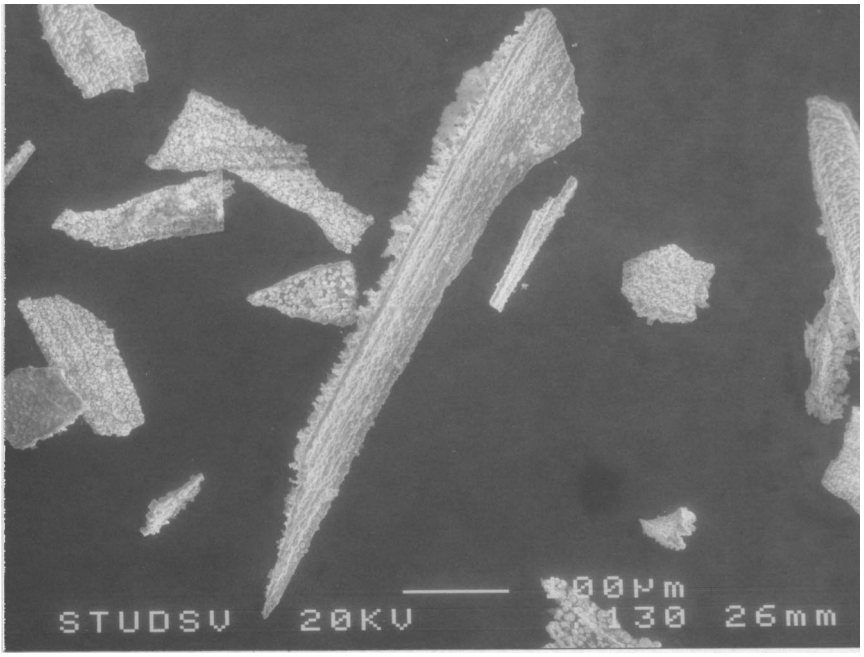

Figure 7
SEM picture of a collection of deposited flakes from the corrosion layer.

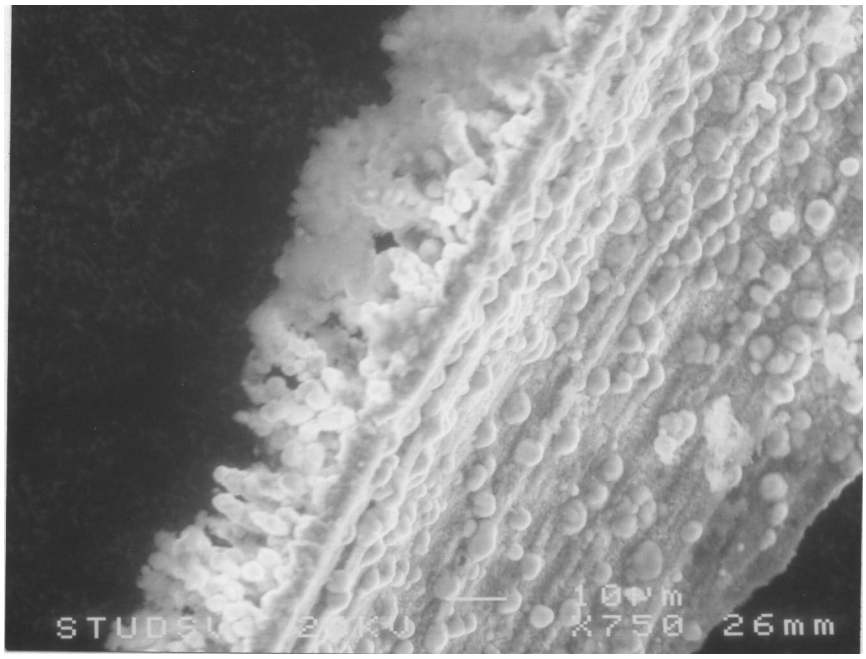

Figure 8
SEM picture at a larger magnification of the center flake seen in Figure 7.

Details of the center flake in Figure 7 are shown in larger magnification in Figure 8.
The "smooth" part of the flake in Figure 8 is sulfur rich and probably consists of sulfide. The dendrites on the left part of the flake probably consist of oxides or carbonates.

Many flakes were point-analyzed in SEM-EDS. The results show that most of them originated from scaled-off sulfur rich strata and that they were double-layered. On top of the sulfide layer was an oxide or carbonate layer (stratum) with dendritic structure. See Figure 8. A SEM-EDS point analysis of the sulfide part is shown in Appendix A, Figure A7. The sulfide part has been oriented towards the metal. It was rather smooth and had imprints of the structure of the metal surface. The result of a point analysis in SEM-EDS of the dendrites is shown in Appendix A, Figure A8. It is indicated that the dendrites probably consist of oxides and/or carbonates. No sulfur was found in dendrites.

There is Si, Al, Mg and Ca found in both strata of the flakes. However, although present in solution, there is no chlorine at all found in the flakes. Si was in the solution and was also incorporated in the flakes. Al, Mg and Ca also originate from the solution. In some flakes no sulfur was found at all. They were probably pure oxide or carbonate flakes. Flakes with and without a sulfur-containing stratum look the same in SEM. They have a smooth side and a dendritic side. The difference between them is probably that separation has occurred between sulfide and oxide strata in one type and not in the other. In Figure 9 a case is shown in which investigations were performed with SEM-EDS on both sides of the needle-shaped flake. EDS-spectra from the point analyzes are

shown in Appendix A, Figures A9 (up-side) and A10 (down-side). The flake was rotated between analyzes in order to analyze both sides.

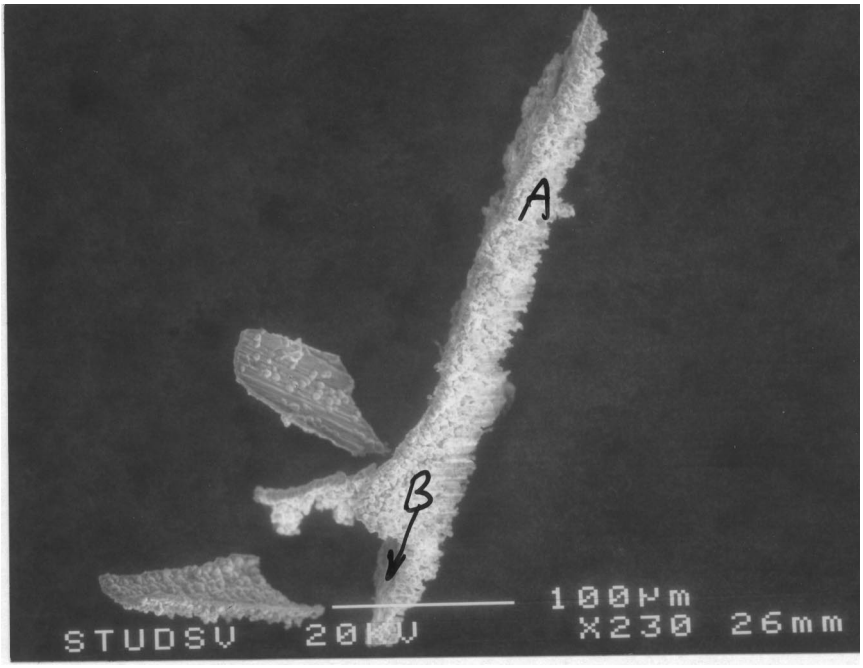

Figure 9
A needle-like flake analyzed on both sides in SEM-EDS.

The needle-like flake consists of oxide and/or carbonate and also the dendrites growing on it. The underside is smooth and has probably been attached to a sulfide sub-layer before detaching. The dendritic, upper side has probably faced the solution. The two smaller flakes in Figure 9 are double layered and have the sulfide sides turned upwards.

A special search for root parts or substrate areas of whiskers was performed. However, the result of this was meager. It was not possible to find places in corrosion layers remaining on the metal or detached as flakes that could uniquely be pointed out as whisker root-areas. Such areas were also searched in the cross section sample. Beside numerous small pits there were areas found of local broad pitting attacks with oxide closest to the metal. It was, however, not possible to judge whether these two kinds of pitting attacks had any close relation to the whisker growth. In all areas with pits, the outer strata had scaled off. This could be a reason for that no signs of whisker-roots were seen and this phenomenon could also explain why the whiskers fell off so easily. It should be commented here that the observed oxide/carbonate dendrites on corrosion layers and detached flakes probably are the origin of the full sized whiskers.

SEM-EDS of whiskers

Whiskers or needle-shaped crystals grew from the surface of the sample throughout the exposure. They were rather numerous and were easily seen by the naked eye.

At the end of the exposure, the sample was carefully extracted from the solution and stored in a way to protect the whiskers from damage. However, afterwards it was difficult to find good whiskers to investigate. This is because they are very fragile, easily cracked and detached from the sample surface at extraction from the solution. An example of whiskers found on the surface is shown in Figure 10.

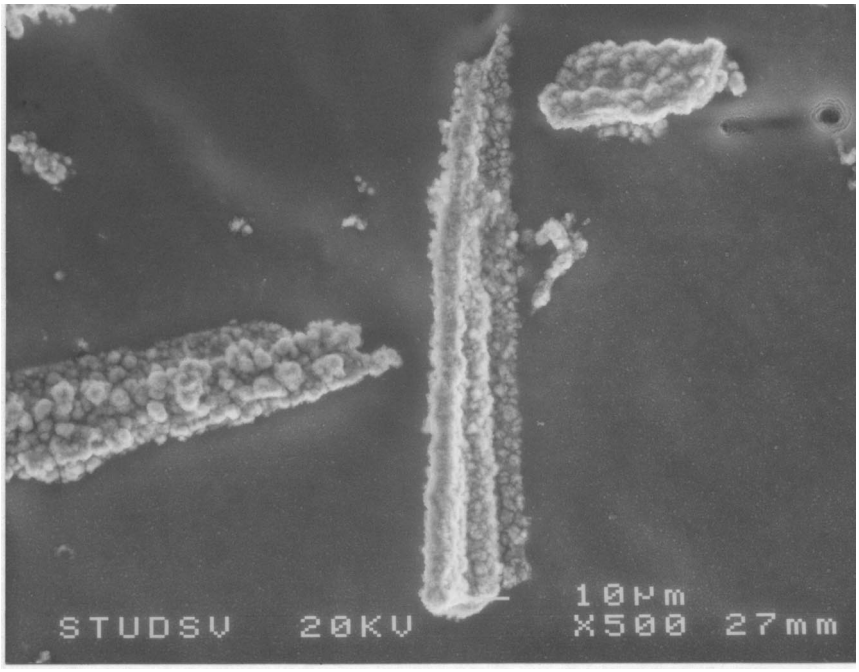

Figure 10
Whiskers found on the sample surface.

Point analysis with SEM-EDS was performed in different parts of the whisker shown in the middle of Figure 10. The result shows that the whisker has a core of sulfide, see Appendix A, Figure A11. It was also found that the composition ratio of sulfur to copper increases from the root to the top part of the whisker.

There were straight flange edges along the sides of the whisker, as can be seen in Figure 10. The analyses show that the sulfur content in the flanges was low and that they probably consist of oxide and/or carbonate.

X-ray diffraction of whiskers

In order to investigate the composition further and to get some information on the structure of the material in the surface film and of the whiskers, X-ray diffraction analysis was performed on some whisker material and pieces of the surface. The somewhat unexpected result is that no crystalline sulfides were found in the whiskers and in the surface film. The investigation was performed on different but nevertheless similar material originating from another exposure [5] than the one accounted in the present investigation. This has to be remembered when interpreting the results.

The diffraction lines consist of some sharp and some more diffuse lines. The lines match crystals of copper(I)oxide, copper(II)oxide, and copperhydroxide, see Tables 2 and 3. All observed lines can be explained with these three phases.

Table 2
X-ray diffraction lines; d-values and relative intensities for a black surface film. Listed d-values and relative intensities for $Cu(OH)_2$, Cu_2O and CuO taken from the database [10].

Observed d-values (I)*	$Cu(OH)_2$ d (I) JCPDS 35-0505	Cu_2O d (I) JCPDS 5-0667	CuO d (I) JCPDS 5-0661
5.30 (3)	5.29 (80)		
3.72 (2)	3.73 (90)		
3.020 (4)		3.02 (9)	
2.75 (3)			2.751 (12)
2.72 (1)			
2.60 (3)	2.63 (100)		
2.53-2.51 (46)	2.50 (60)		2.530 (49) 2.523 (100)
2.465 (100)		2.465 (100)	
2.39 (1)	2.36 (50)		
2.336-2.308 (49)			2.323 (96) 2.312 (30)
2.274 (2)	2.266 (70)		
2.210 (<1)			
2.135 (26)		2.135 (37)	
1.873 (3)			1.866 (25)
1.711 (2)	1.718 (70)		1.714 (8)
1.509 (20)		1.510 (27)	1.505 (20)
1.410-1.404 (5)			1.418 (12) 1.410 (15)
1.377 (2)			1.375 (19)
1.288 (9)		1.287 (17)	
1.231 (3)		1.233 (4)	

Table 3
X-ray diffraction lines; d-values and relative intensities for whisker material. Listed d-values and relative intensities for $Cu(OH)_2$, Cu_2O and CuO taken from the database [10].

Observed d-values (I)*	$Cu(OH)_2$ d (I) JCPDS 35-0505	Cu_2O d (I) JCPDS 5-0667	CuO d (I) JCPDS 5-0661
5.31 (5)	5.29 (80)		
3.72 (5)	3.73 (90)		
2.75 (5)			2.751 (12)
2.61 (4)	2.63 (100)		
2.53-2.50 (55)	2.50 (60)		2.530 (49) 2.523 (100)
2.35-2.29 (100)			2.323 (96) 2.312 (30)
2.274(2)	2.266 (70)		
1.885-1.886 (9)			1.886 (25)
1.719-1.704 (5)	1.718 (70)		1.714 (8)
1.414-1.405 (9)			1.418 (12) 1.410 (15)
1.379-1.374 (5)			1.375 (19)

* When an interval is given for the d-value it means the diffraction line is broad and diffuse. The intensity value is then the integrated values across the line. Intensities are relative with the largest peak set to 100.

Sulfide could possibly be present if the crystals are extremely small or if the material is amorphous as it could be as a result of rapid, dendritic growth and therefore does not diffract the X-rays. For comparison with the measured diffraction lines presented in Tables 2 and 3, the most intense diffraction lines for all Cu-S phases found in the database are given in Table 4.

Table 4
X-ray diffraction lines; d-values and relative intensities for Cu-S phases taken from the database [10]. Only four of the most intense lines are shown in the table.

Phase	Lines, d-values (relative intensity)	JCPDS ref.no.
CuS	2.81 (100), 1.90 (75), 3.05 (65), 2.72 (55)	06-0464
$Cu_{1.96}S$	2.02 (100), 2.85 (60), 1.72 (60), 3.30 (30)	12-0174
Cu_7S_4	1.94 (100), 2.37 (90), 1.86 (90), 2.86 (75)	23-0958
$Cu_{1.8}S$	1.97 (100), 2.78 (45), 3.21 (35), 1.68 (20)	23-0962
$Cu_{7.2}S_4$	1.97 (100), 2.79 (68), 3.22 (40), 1.68(14)	24-0061
Cu_9S_5	1.96 (100), 2.95 (31), 3.20 (30), 3.04(24)	26-0476
β-Cu_2S	1.98 (100), 1.88 (98), 2.40 (88), 1.71 (45)	26-1116
$Cu_{1.96}S$	2.74 (100), 2.30 (80), 1.99 (40), 1.88 (35)	29-0578
$Cu_{1.92}S$	2.82 (100), 2.31 (100), 2.08 (100), 2.00 (100)	30-0505
CuS_2	2.89 (100), 1.74 (57), 2.05 (42), 2.59 (30)	32-0348
Cu_7S_4	1.96 (100), 2.78 (55), 3.22 (40), 1.95 (40)	33-0489
Cu_2S	1.88 (100), 2.40 (70), 1.97 (70), 2.41 (50)	33-0490
Cu_8S_5	3.13 (100), 1.92 (50), 1.64 (30), 1.11(20)	33-0491
CuS_2	2.81 (100), 1.70 (45), 1.99 (40), 3.25 (30)	33-0492
$Cu_{31}S_{16}$	1.96 (100), 1.87 (95), 2.39 (85), 3.76 (20)	34-0660
Cu_9S_8	1.90 (100), 3.06 (55), 2.77 (45), 1.73 (15)	36-0379
$Cu_{39}S_{28}$	1.91 (100), 3.08 (85), 2.78 (30), 1.82 (30)	36-0380
$Cu_{1.81}S$	1.97 (100), 2.75 (73), 2.00 (61), 2.31 (58)	41-0959
$Cu_{31}S_{16}$	2.39 (100), 2.38 (95), 3.40 (40), 3.36 (30)	42-0564
β-Cu_2S	1.98 (100), 1.89 (70), 2.41 (57), 1.71 (35)	46-1195

LRS on whiskers

Most LRS spectra recorded are accounted in collection figures in Appendix B. For evaluation, the spectra were compared with reference spectra of prepared samples of CuO (Appendix B, Fig. B8), Cu_2O, CuS (Appendix B, Fig. B7) and Cu_2S.

The LRS investigation was performed in the following way:

- One typical whisker was selected for detailed investigations.
- A selection of 10 other whiskers was investigated by one spectrum each in order to collect statistical information.
- A part of the exposed copper cylinder was "scraped" and the scraped section of the corrosion product layer was investigated in detail.
- Some flakes of the detached corrosion product layer were investigated.
- A cross section of such a flake was investigated in detail.

The whisker selected for a thorough investigation was about 6 mm long and the mean diameter was about 200 µm. A principal drawing, not to scale in detail, is shown in Figure 11. Spectra were recorded from the root part along the middle of the whisker to the top part. There was a distance of about 100 µm between each spectrum spot. The spectra recorded are all shown in Appendix B, Figure B1.

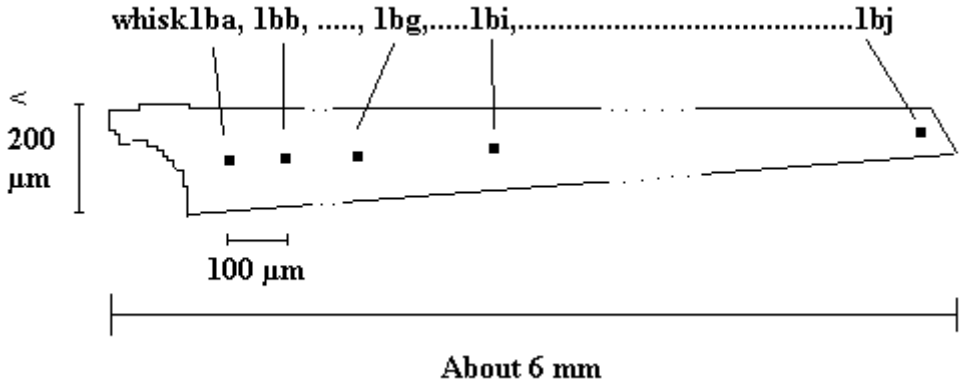

Figure 11
Position of recorded Raman spectra ("whisk1ba", etc.) on the whisker examined in detail. Figure not to scale.

It can be seen in Figure B1 that essentially the same appearance of the spectra was observed all over the body of the whisker (from root to top). The individual position spectra are named whisk1ba – whisk1bg in Figure B1. The tip spectra, whisk1bi and –j

also give the same appearance. The spectra observed are identified as originating mainly from CuO.

A selection of 10 other whiskers, numbered 2-11, was checked by recording one (or in a couple of cases two) spectra per whisker in order to collect statistical information. The maximum length of these whiskers is about 5 mm.

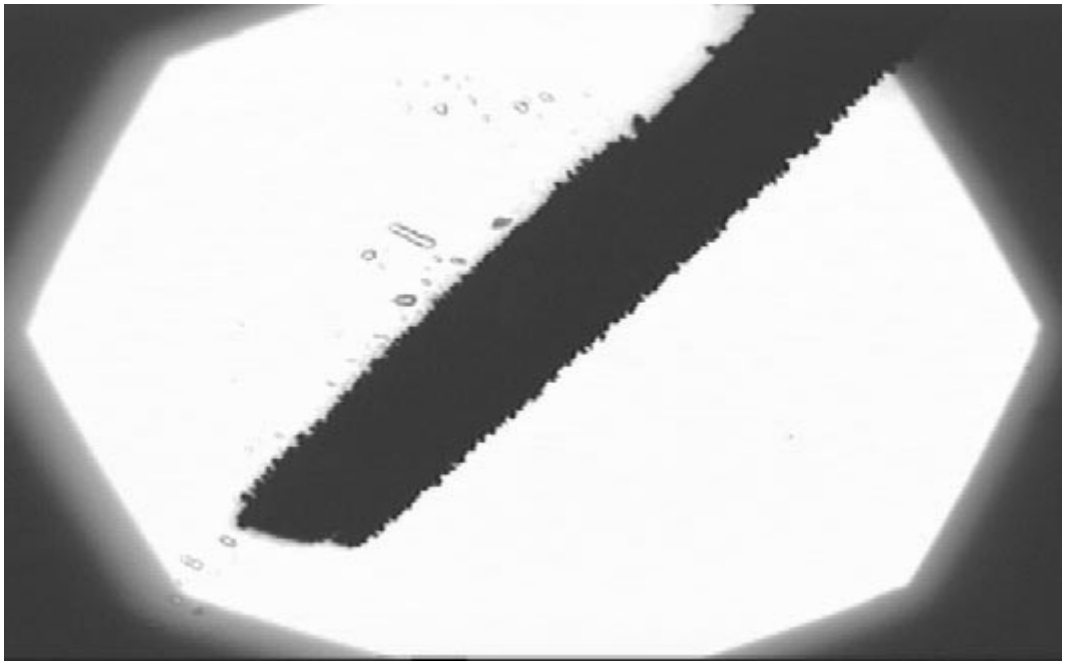

Figure 12
Video-optic picture of whisker selected for LRS. Picture height corresponds to 1.1 mm (X75).

An example of a video-optic picture of such a whisker is shown in Figure 12. The dendritic growth on the flanges of the whisker (as already discussed in the SEM-EDS part above) can be seen in the picture. Most spectra were recorded on a mid-section of the actual whiskers.

All spectra recorded in this series are collected in Appendix B, Figure B2. The same spectrum appearance can be seen in several whiskers but there are also differences. In figure B2 the large peak for the tip part of the whisker originates from CuS. Most other features of the spectra originate from CuO. Some of the recorded spectra are shifted vertically, due to higher background noise.

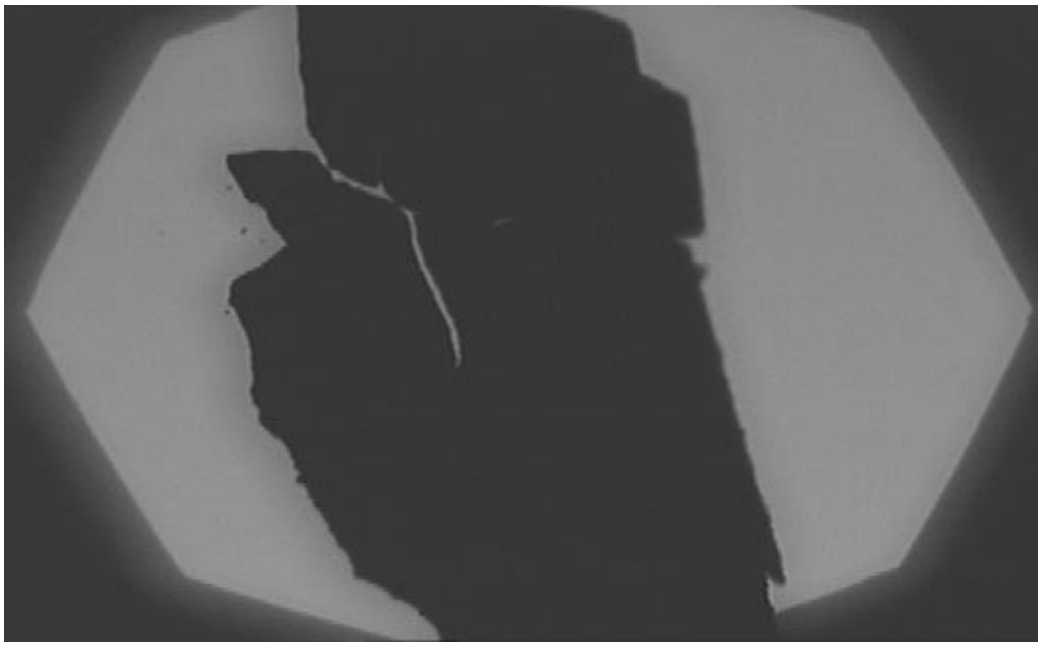

Figure 13
Video-optic picture on detached (scraped) material. Picture height corresponds to 1.1 mm (X75).

A video-optic picture from the detached (scraped) material is shown in Figure 13. An example of the Raman spectra recorded for this scaled-off part of the corrosion layer is shown in Appendix B, Figure B3. The other spectra that were recorded, but are not accounted here, all look the same. The spectrum "Cylavsk2" in Figure B3 was recorded on the smooth dark surface seen in Figure 13. CuO gives this type of spectrum.

The cylinder with corrosion products was grounded down to the metal surface in one area, see the video optic picture in Figure 14. This was done in order to generate a tangential cross section of the corrosion layer and to record Raman spectra from different parts of the cross section.

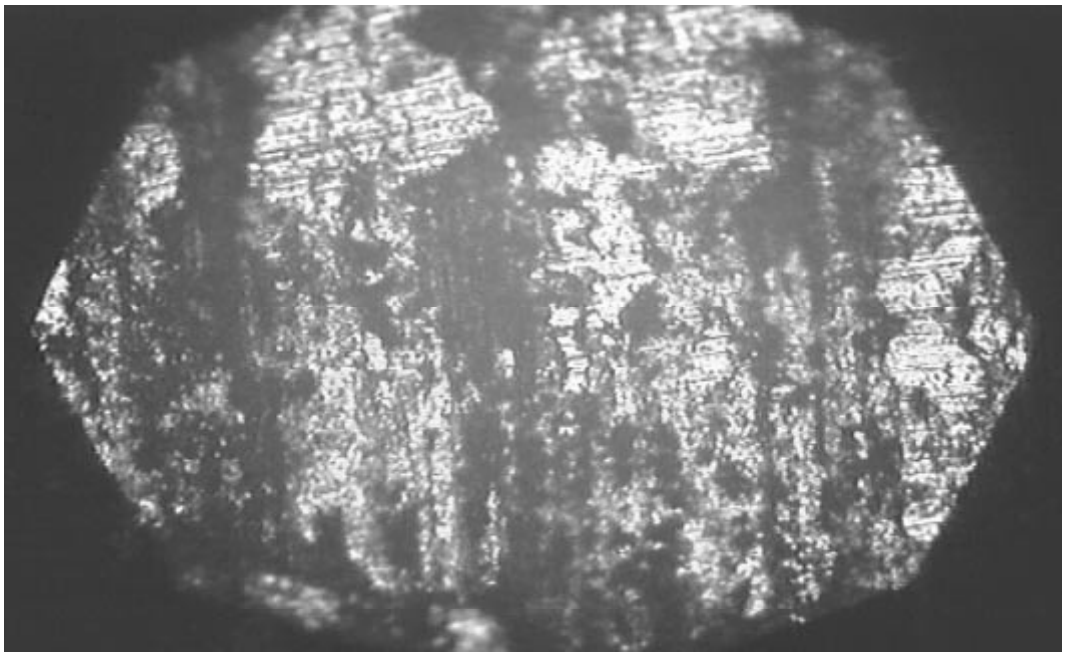

Figure 14
Video-optic picture of the central metallic part of the grounded area. Picture height corresponds to 280 μm (X300).

The LRS analyses made on this surface were performed along a line crossing the area shown in Figure 14 parallel to the short, vertical axis of the picture. A principal drawing (not to scale) of points of analyzes are shown in Figure 15. The positions of whiskers are only marked in the figure. They had fallen off and were not there at the time of analyses.

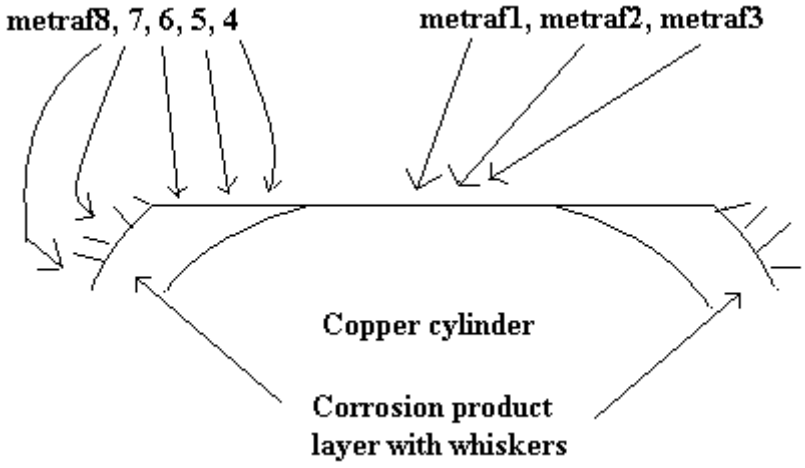

Figure 15
Positions of recorded Raman spectra ("metraf 1-8") on the grounded cylinder surface seen in Figure 14. The figure is not to scale.

The spectra recorded are all collected in the Appendix B, Figure B4. Metraf1 (on metal), metraf2 and metraf3 spectra are recorded on different details in the metallic area. See Figures 14 and 15. The spectra named metraf 4-8 are recorded on the scraped corrosion layer (cross section) and on the un-scraped, outer surface of the corrosion layer. See Figure 15. The spectra in Figure B4 contain elements of CuO and CuS but also from other not clearly identified phases.

One detached flake of the corrosion layer was prepared in such a way that it could be investigated in cross-section perpendicular to the surface. A video-optic picture of this cross section is shown in Figure 16.

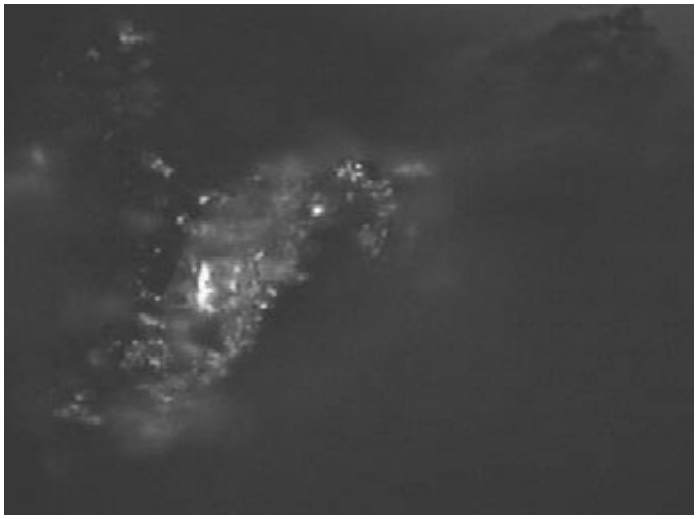

Figure 16
Video-optic picture of the cross section. Picture height corresponds to 280 μm (X240).

The LRS spectra taken on the cross section shown in Figure 16 are accounted in Appendix B, Figures B5 and B6 because there are two different types of spectra.

Tvarsn1(dark part) and 2(light part) are recorded for the central parts of the cross section of Figure 16. These spectra show the presence of CuO. Tvarsn3(dark part) and 4(light part) are recorded on one edge and 5(black part) on the other edge of the cross section. These spectra probably originate from CuS.

Discussion

During the exposure a black layer of corrosion products formed on the sample. This layer or at least part of it was very loosely attached and scaled off in several relatively large areas.

The surface of the corrosion layer as well as a cross section was investigated in a light optical microscope, in SEM-EDS and in LRS. Whiskers found on the surface and those that had sedimented to the bottom of the reaction flask were also investigated with the same methods.

The thickness of the corrosion layer was relatively even around the sample and varied in the range 5 – 25 μm. At least a part of the corrosion layer was subdivided into five parallel strata. There are probably even more strata to be found in other cases. In this case the two outer strata seem to be sulfide layers. The outer stratum could be CuS and the next inner Cu_2S. The inner sulfide stratum adheres poorly to the next stratum, which probably consists of an oxide, probably CuO. Therefore scaling off most often occurs between those two strata.

In the general case there is probably also an oxide and/or carbonate stratum outside of the sulfide strata. This is observed in some cases. On top of this outermost stratum growth of dendrites is often observed. It is therefore concluded that the order of strata in the corrosion layer could be as follows. An outermost growth of oxide/carbonate dendrites followed by an oxide/carbonate stratum, thereafter a CuS stratum, a Cu_2S stratum and finally a couple of oxide strata, perhaps CuO and finally Cu_2O closest to the metal. This picture of stratification and order of strata was partly verified by the different methods of investigation. The scaling off tendency of the corrosion layer is probably a result of bad bonding between sulfide and oxide strata.

There were pitting attacks found in several places. There was a multitude of small pits but also of shallow pits with a larger radius. The corrosion layer was about 4 times thicker (about 20 μm) in these areas and the sulfide had always scaled off in the vicinity of pits. There was no chlorine found in the oxide filled pits and therefore the mechanism of pit formation should be quite different from the mechanism normally proposed for copper pitting in saline waters. Since the sulfide layer had scaled off in the vicinity of pits and no whiskers were found intact on the surface at the examination there may be a connection between pits and whisker growth.

During the time of exposure there were numerous whiskers to be seen on top of the corrosion layer. They were about 5-10 mm long at the end of the exposure and very fragile. Therefore, despite very careful handling, it was very difficult to find any whiskers on the surface after interruption and drainage of the experiment. A few broken whiskers were found on the surface and a multitude on the bottom of the reaction vessel.

SEM-EDS analyses clearly demonstrated that whiskers have a core of sulfide and that the sulfide contents increases from the root to the tip of the whisker. There were flanges

in several places around a whisker and they were parallel with each other and the long axis of the whisker. The sulfide contents of the flanges as well as on other outer parts of the whisker was very low. The phases occurring there should therefore be an oxide and/or a carbonate. This general picture of the anatomy of a whisker was also verified by LRS in which CuO, CuS and probably also a carbonate were observed. The stratified structure of whiskers in a way reminds of the stratification of the corrosion layer. However, the corrosion layer has a plane geometry the whisker geometry of strata is concentric cylindrical. Roots of whiskers were searched for on the corrosion layer without any unique result. However, it could be speculated whether the numerous pits could be the bottom part of such a root area.

The question if whisker growth is due to localized or general corrosion thus remains. It is therefore of interest to suggest other experiments that may give the answer.

One method would be to restrict the supply of oxygen in the experiment. The absence of this electron sink will disfavor general corrosion and favor localized attacks, which are less oxygen consuming. If the visual surface coverage by whiskers is changed by these conditions it may be a part of general corrosion. However, if the coverage remains about the same as with oxygen, the coverage may reflect the number of local corrosion pits.

A more elaborate method would be to try to support the whiskers or, in this case rather, some other shape of dendrites, by letting them grow in a porous or viscous medium applied on a flat copper surface. An obvious choice of such a medium would be bentonite clay, the material selected as backfill material between the canisters and the host rock in the proposition for a final disposal of the spent nuclear fuel. At the termination of such an experiment the clay is cut at the copper interface. The surfaces are then examined for a correlation between positions of corrosion pits at the copper surface and of dendrite/whisker growth into the clay. In order to verify dendrite/whisker growth into the clay, several consecutive slices of clay may be investigated.

It was found in the present experiments that the development of the corrosion layer and the whisker growth was rapid during the first month of the experiment but thereafter it seemed to slow down or even stop. It can therefore be suspected that the limited source of sulfide in the reaction vessel was exhausted. Although no water analyses were made of the sulfide concentration, an estimation of the sulfur consumption can nevertheless be made by a simple mass balance calculation. With the aid of the SEM picture of the different strata of the corrosion layer in Fig. 4 the thickness of the sulfide-containing layer is estimated to 2.5 μm (corresponding to 1 cm in Fig. 4). Then, by the assumption of an equally thick layer on the sample cylinder surface (Fig. 1), the volume of the layer can be estimated to $3.5 \cdot 10^{-9}$ m^3. Finally, by assuming an average copper (I/II) sulfide density of 5 kg/L, the total mass of the sulfide layer is estimated to 0.02 g which corresponds to $2 \cdot 10^{-4}$ moles of CuS or to $1 \cdot 10^{-4}$ moles of Cu_2S. The estimated figures can be compared with the initial amount of sulfide in the reaction vessel, which is $6 \cdot 10^{-4}$ moles. The used literature value for density refers to crystalline copper sulfides and it is probably too large for the partly amorphous phases found here, which may give an over-estimation of the amount of sulfur in the corrosion layer. On the other hand, the sulfide

layer occasionally scaled off during the experiment and several sulfide layers may have developed consecutively on the same area of the sample. Moreover, the whiskers are not included in the mass balance. The conclusion is therefore that the corrosion was probably limited by the source of sulfide in the reaction vessel solution.

Finally, the consequences of whisker growth for the long-term copper canister integrity in a Swedish deep underground final repository of spent nuclear fuel can be speculated about to a limited extent. In the reducing, sulfide-rich environment that is expected to prevail for long periods in a deep underground repository, a general corrosion of copper to coppersulfides will take place if an electron sink, alternative to oxygen, is present. The alternative sink could, for example, be Fe(III) or polysulfides. The copper sulfides will not form a passive layer, so the corrosion will proceed. The corrosion rate may then be controlled by the access of sulfide and electron-acceptor from the environment, diffusing through the bentonite clay, or from the clay itself. The diffusion paths will be shortened by the growth of dendrites into the clay. Localized corrosion would pose a more severe threat, since canister penetration will then occur in a much shorter time. However, as pointed out earlier, the question whether the dendrite growth is connected with localized pitting corrosion or a part of general corrosion is still open.

Summary and conclusions

- The corrosion layer is stratified and consists of separate strata of copper oxides, sulfides and carbonates. The carbonates are not verified.
- Phases observed at LRS are (Cu_2O), CuO, CuS, another copper sulfide (Cu_2S?) and perhaps copper carbonate.
- Scaling off of a part of the corrosion layer occurs very easily and preferably between sulfide and oxide layers.
- Numerous whiskers grew on top of the corrosion layer in this case.
- Whiskers are also stratified but in a concentric, cylindrical way.
- On whiskers and on top of the corrosion layer there are small dendrites. These could be the starting points for whisker growth.
- No specific root areas of whiskers were found. However, it could be speculated whether the numerous pits could be the bottom part of such a root area.
- The pitting mechanism is different from the one normally observed on copper in a saline environment since there was no chloride present in the corrosion products.
- There is probably a core of probably amorphous sulfide in a whisker. Perhaps this is acting as a rapid route of transportation for copper from the surface of the underlying metal and out to the growing parts of the whisker.
- In order to clearly demonstrate a relation between whisker growth and local corrosion an experiment with supported whiskers could probably be used.
- The corrosion was probably limited by the source of sulfide in the reaction vessel solution.

Acknowledgements

This project was commissioned and financed by SKI, which is gratefully acknowledged. The authors thank Mrs. Christina Lilja of SKI, who was the contact person for this work, for many fruitful discussions.

References

1. Engman, U. och Hermansson, H-P. Korrosion av kopparmaterial för inkapsling av radioaktivt avfall – En litteraturstudie. SKI Rapport 94:6 (1994).

2. Hermansson, H-P. Some properties of copper and selected heavy metal sulfides. A limited literature review. SKI Report 95:29 (1995).

3. Eriksson, S. and Hermansson, H-P. Pitting corrosion of copper in nuclear waste disposal environments. SKI Report 98:2 (1998).

4. Hilden, J., Laitinen, T., Mäkelä, K., Saario, T. and Bojinov, M. Surface films and corrosion of copper. SKI Report 99:27 (1999).

5. Hermansson, H-P. and Eriksson, S. Corrosion of the copper canister in the repository environment. SKI Report 99:52 (1999).

6. Laitinen, T., Mäkelä, K., Saario, T. and Bojinov, M. Susceptibility of copper to general and pitting corrosion in highly saline groundwater. SKI Report 01:2 (2001).

7. Beverskog, B. and Puigdomenech, I. Revised Pourbaix diagrams for copper at 5-150°C. SKI Report 95:73 (1995).

8. Hermansson, H-P. och Beverskog, Björn. Gropfrätning på kopparkapsel. SKI Rapport 96:25 (1996).

9. Beverskog, B. and Puigdomenech, I. Pourbaix diagrams for the system copper-chlorine at 5-100°C. SKI Report 98:19 (1998).

10. PDF-2 Database version 2.16. JCPDS International Center for Diffraction Data, Newton Square, USA.

Appendix A
SEM-EDS spectra.

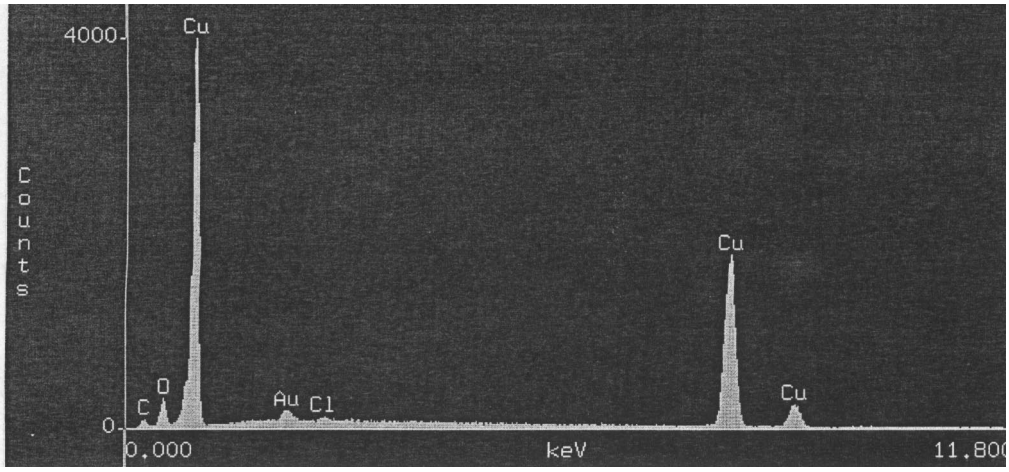

Figure A1
SEM-EDS point analysis in the inner stratum, A. See Figure 4.

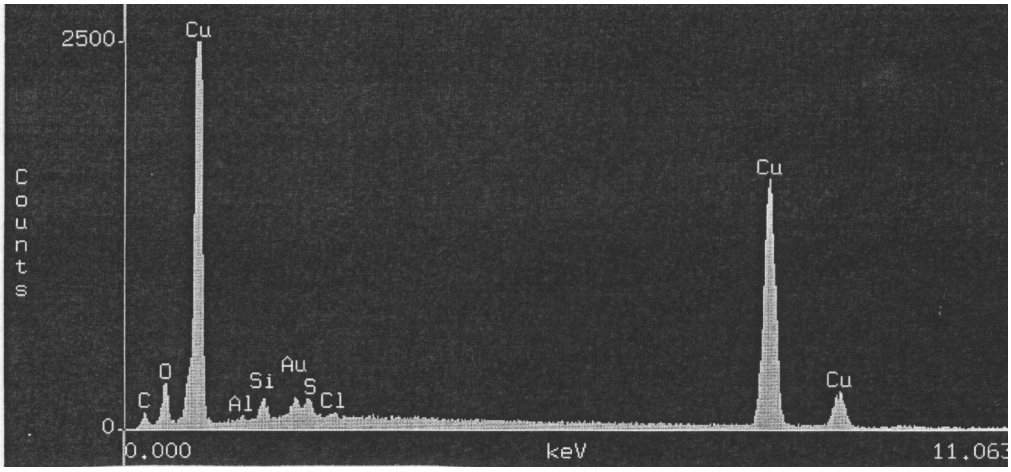

Figure A2
SEM-EDS point analysis in the second inner stratum, B. See Figure 4.

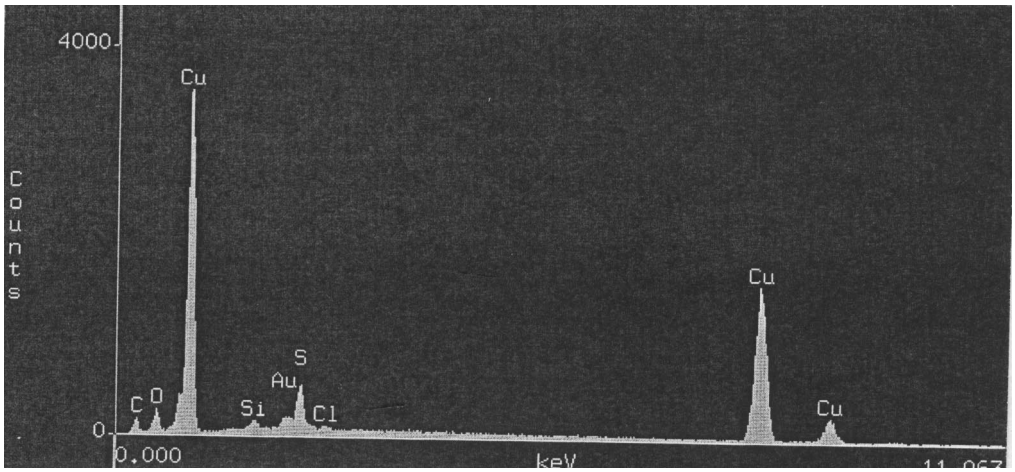

Figure A3
SEM-EDS point analysis in the next outer stratum, C. See Figure 4.

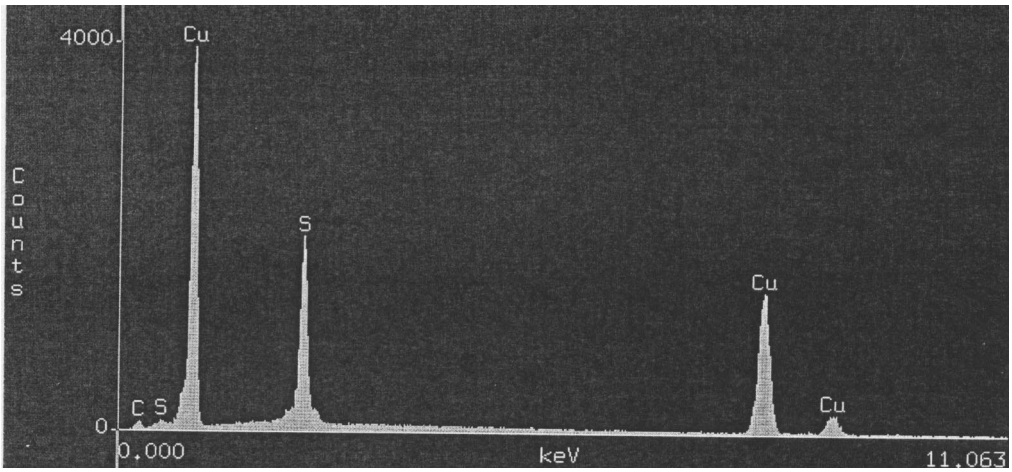

Figure A4
SEM-EDS point analysis in the outer stratum, D. See Figure 4.

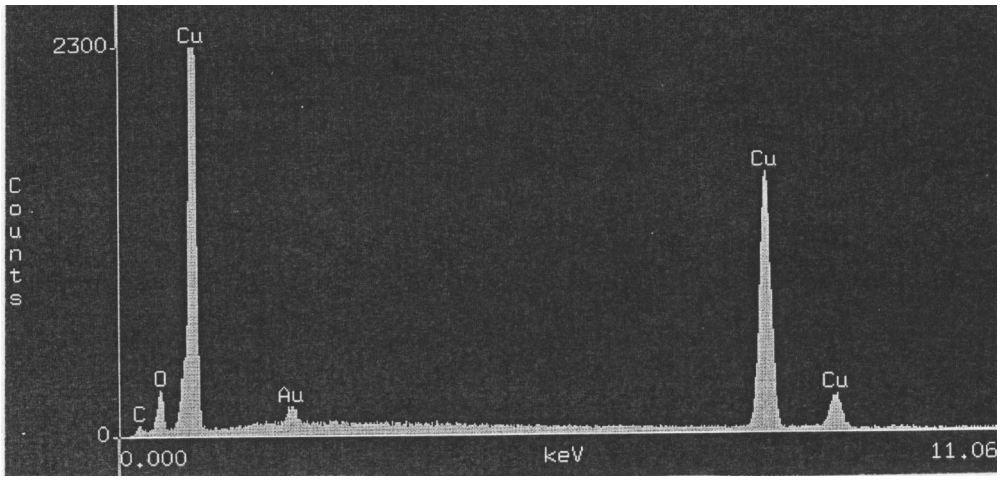

Figure A5
SEM-EDS point analysis in the bottom of the pit, area A. See Figure 5.

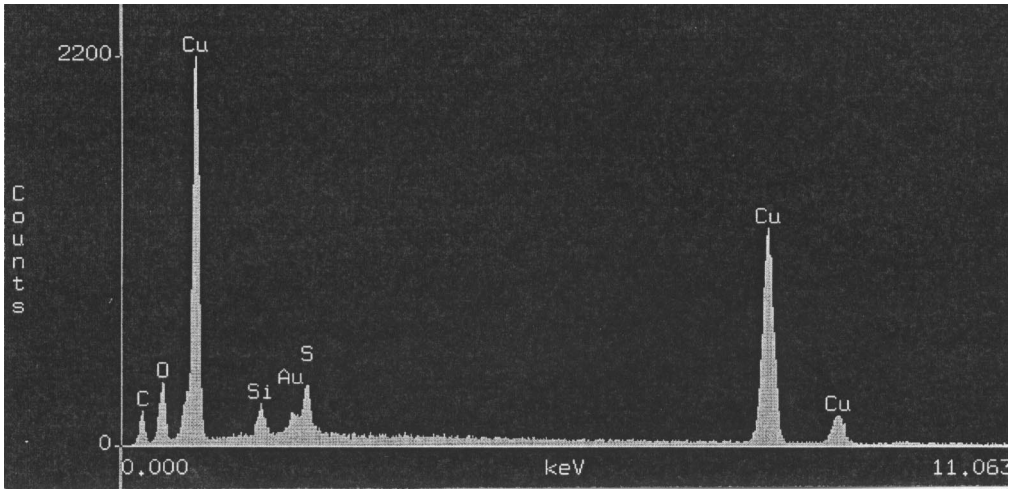

Figure A6
SEM-EDS point analysis in the bottom of the pit, area B. See Figure 5.

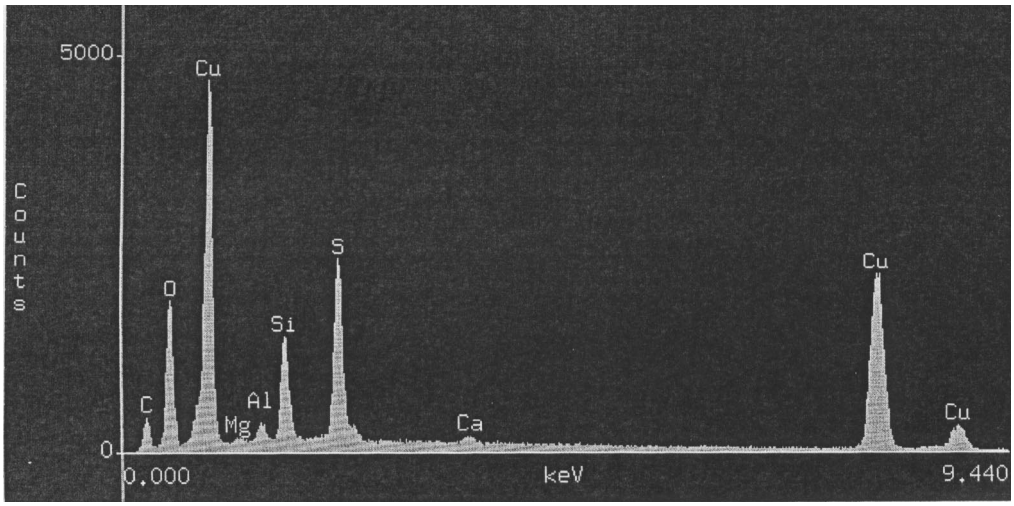

Figure A7
SEM-EDS point analysis of the smooth sulfide part of the flake shown in Figure 8. The sulfide part has been oriented towards the metal.

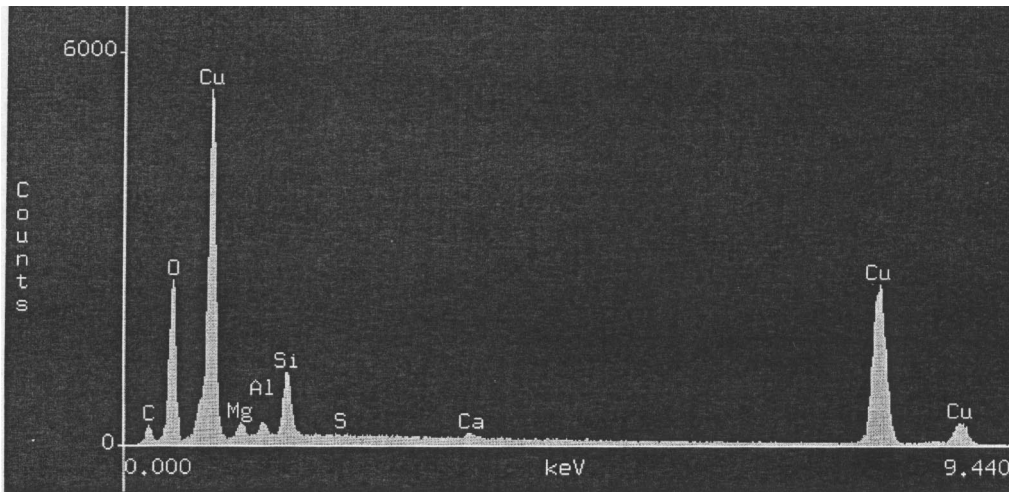

Figure A8
SEM-EDS point analysis of the dendrites on the flake shown in Figure 8. The dendrites faced the solution.

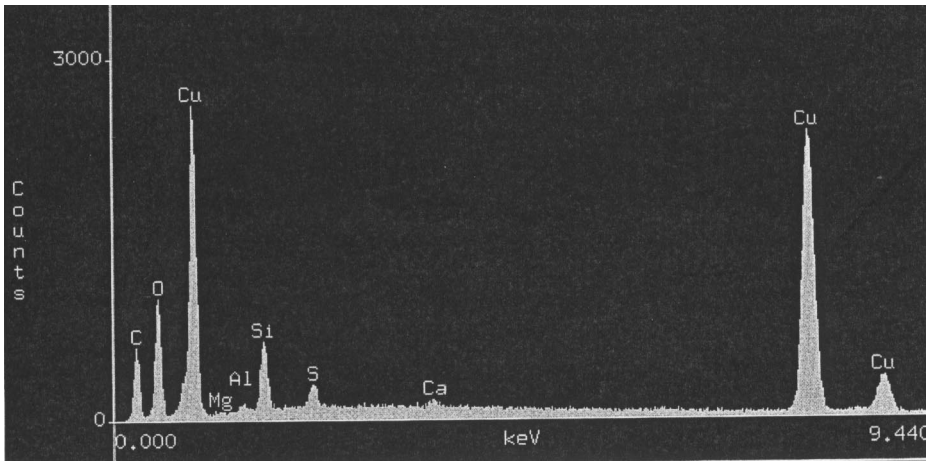

Figure A9
Point analysis of the dendritic side of the flake in Figure 9.

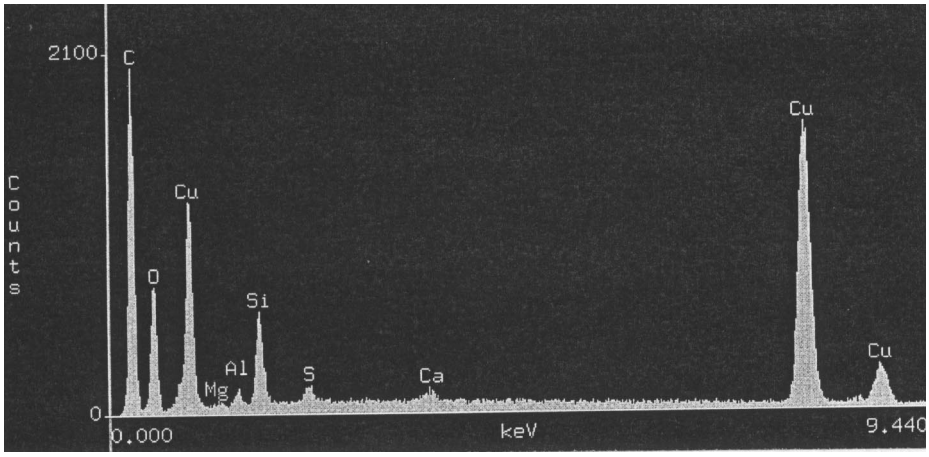

Figure A10
Point analysis of the smooth side of the needle like flake in Figure 9.

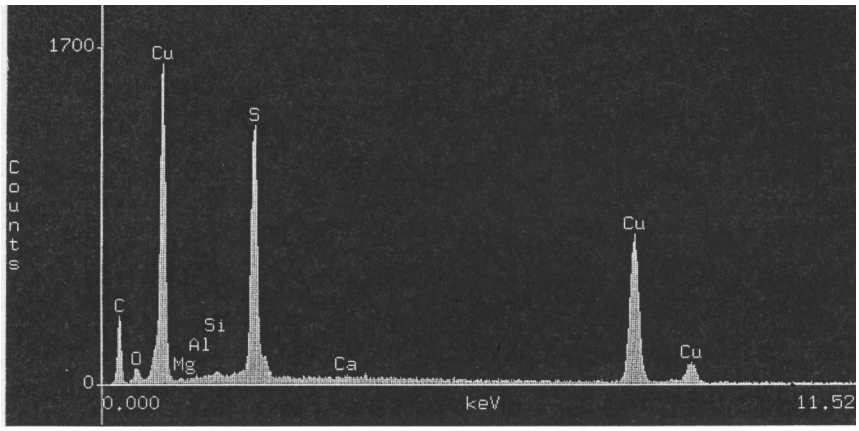

Figure A11
SEM-EDS point analysis of the core part of the whisker shown in Figure 10.

Appendix B

LRS spectra

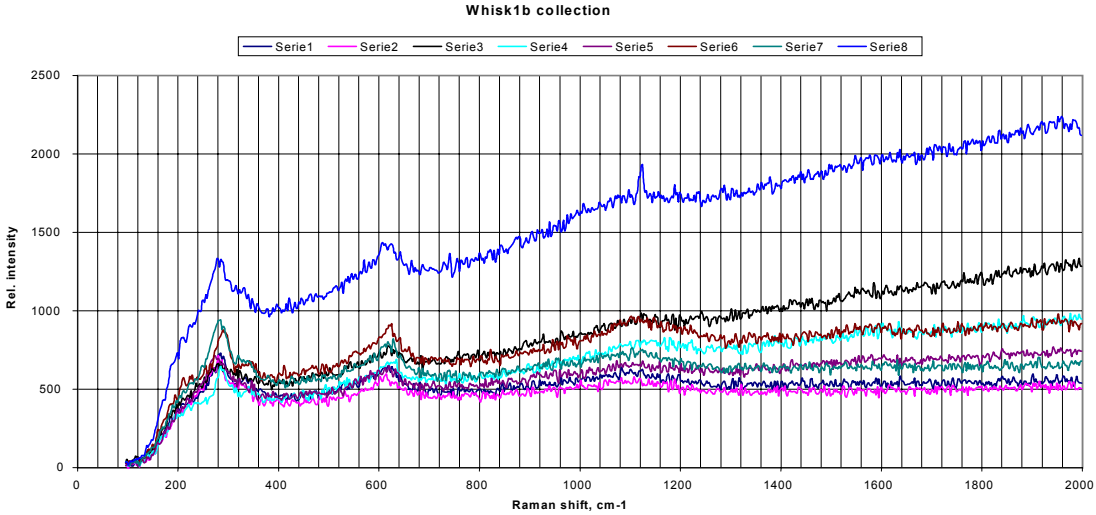

Figure B1 Raman spectra of whisker. Recorded at indicated positions of the whisker schematically drawn in Figure 11. Legend: Serie 1= Whisk1ba, Serie 2= Whisk1bb, Serie 3= Whisk1bc, Serie 4= Whisk1bd, Serie 5= Whisk1be, Serie 6= Whisk1bg, Serie 7= Whisk1bi, Serie 8= Whisk1bj.

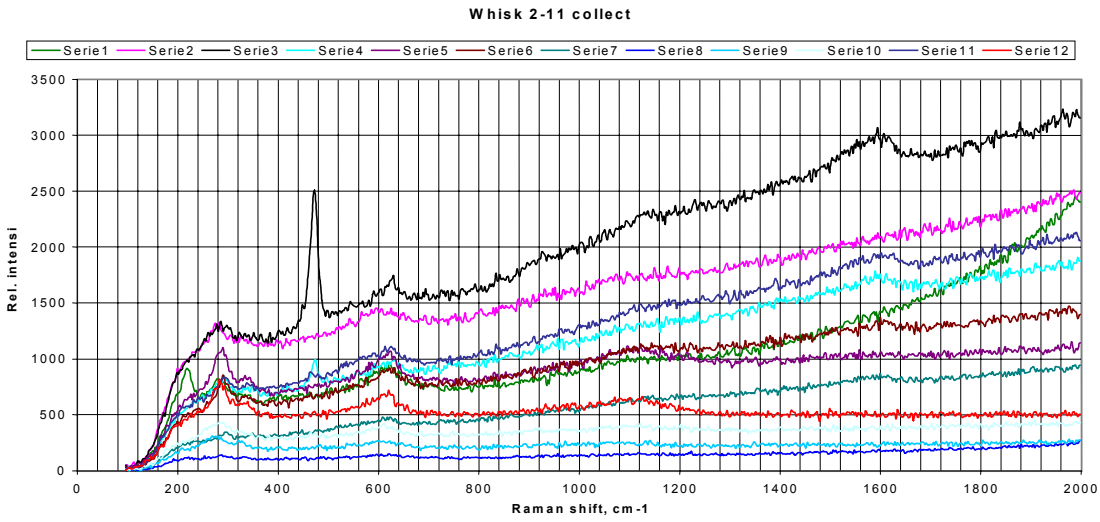

Figure B2 Raman spectra recorded at indicated positions in the selected whiskers. Legend: Serie 1= Whisk2a (light part), Serie 2= Whisk2b (dark part), Serie 3= Whisk3a (tip), Serie 4= Whisk3b (mid part), Serie 5= Whisk4a (tip), Serie 6= Whisk5a (mid part), Serie 7= Whisk6a (mid part), Serie 8= Wwhisk8a (mid part), Serie 9= Whisk9 (mid part), Serie 10= Whisk10 (mid part), Serie 11= Whisk11a (mid part), Serie 12= Whisk11b (mid part).

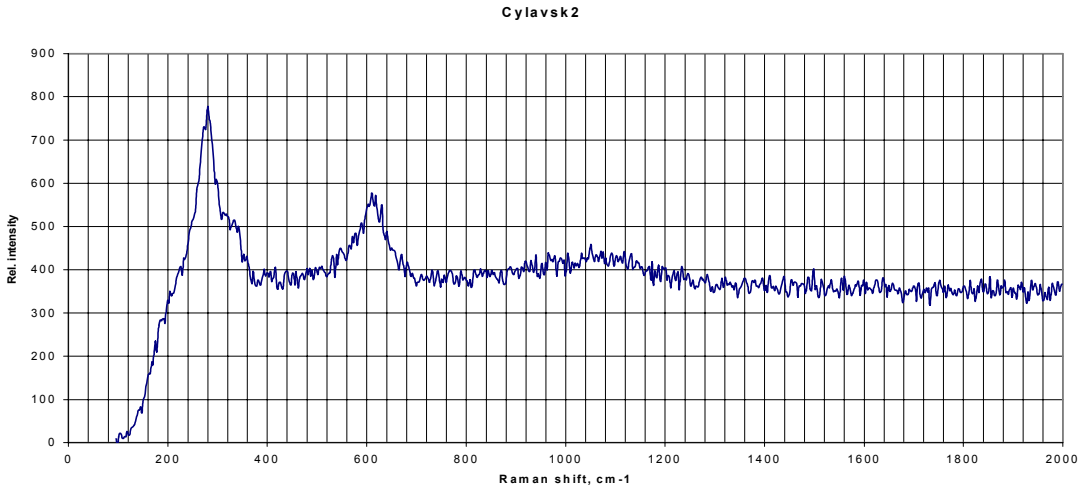

Figure B3
Example of the Raman spectra recorded for the scaled-off part of the corrosion layer shown in Figure 13.

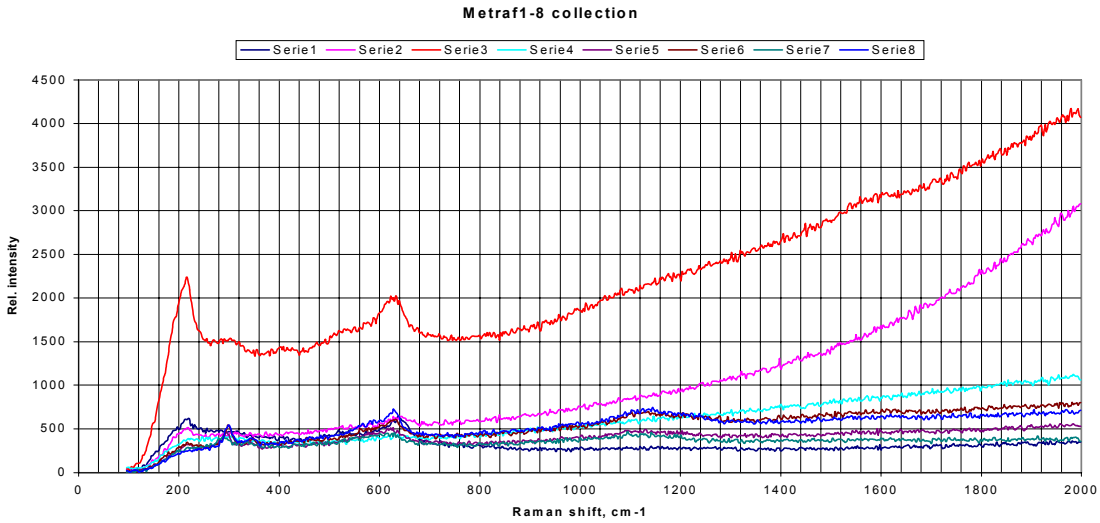

Figure B4
Collection of Metraf spectra. Legend: Serie 1= metraf1, Serie 2= metraf2, Serie 3= metraf3, Serie 4= metraf4, Serie 5= metraf5, Serie 6= metraf6, Serie 7= metraf7, Serie 8= metraf8.

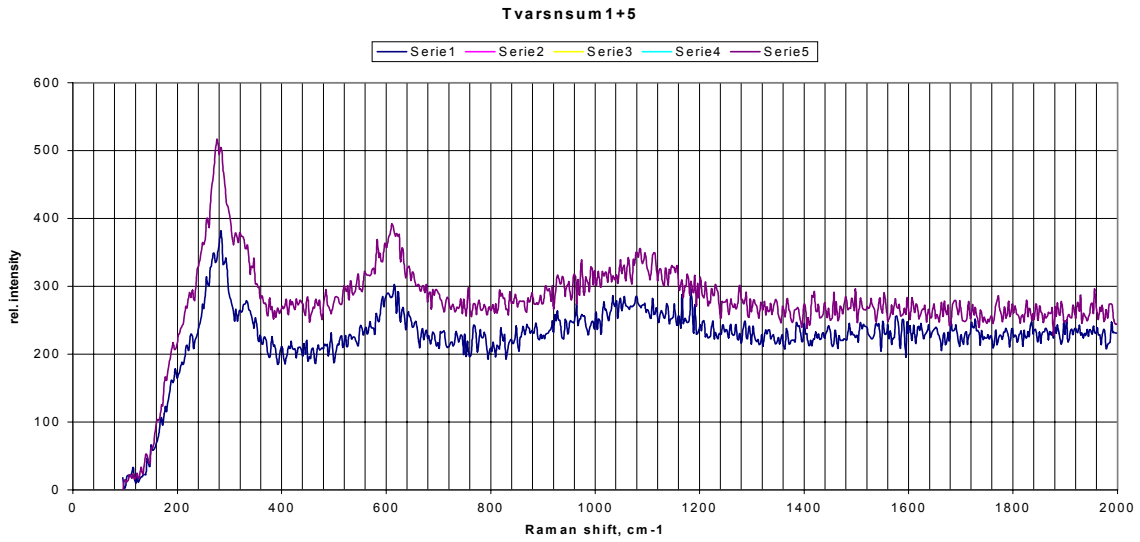

Figure B5
Collection of tvarsn spectra A. Legend: Serie 1= tvarsn1, Serie 5= tvarsn5.

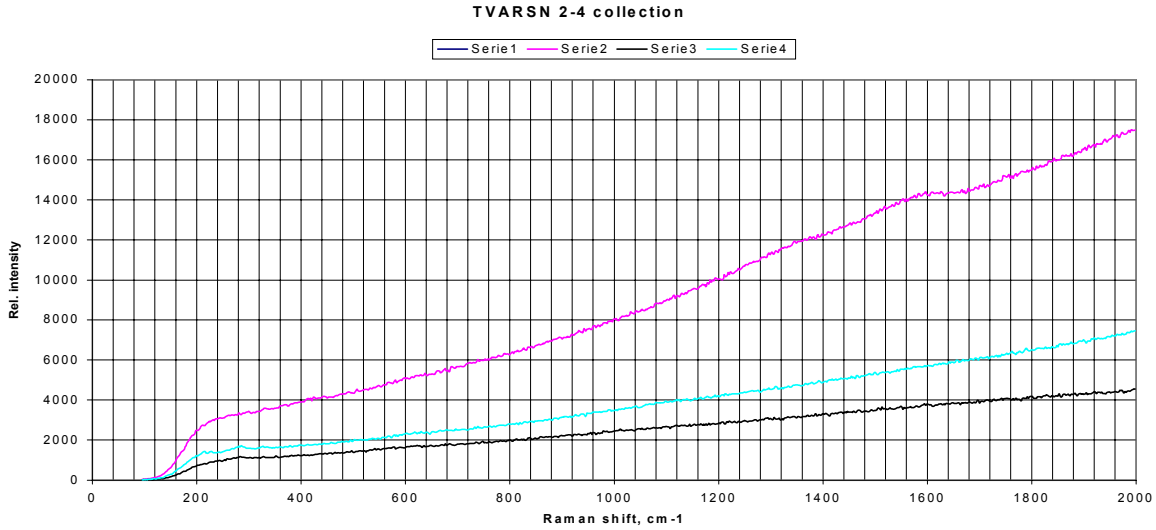

Figure B6
Collection of tvarsn spectra B. Legend: Serie 2= tvarsn2, Serie 3= tvarsn3, Serie 4= tvarsn4.

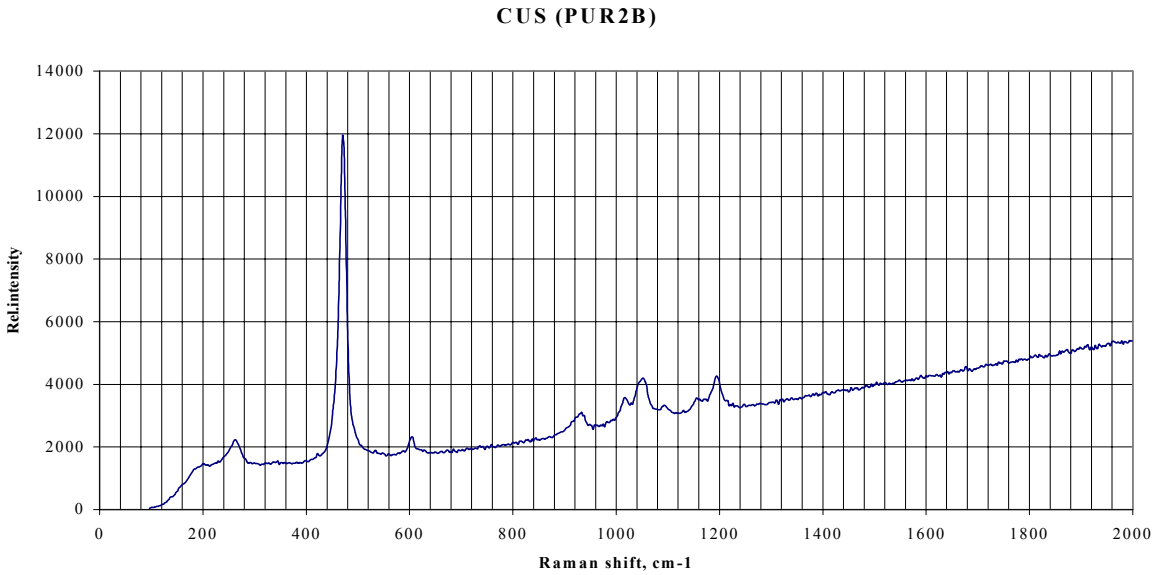

Figure B7
Reference spectrum of CuS.

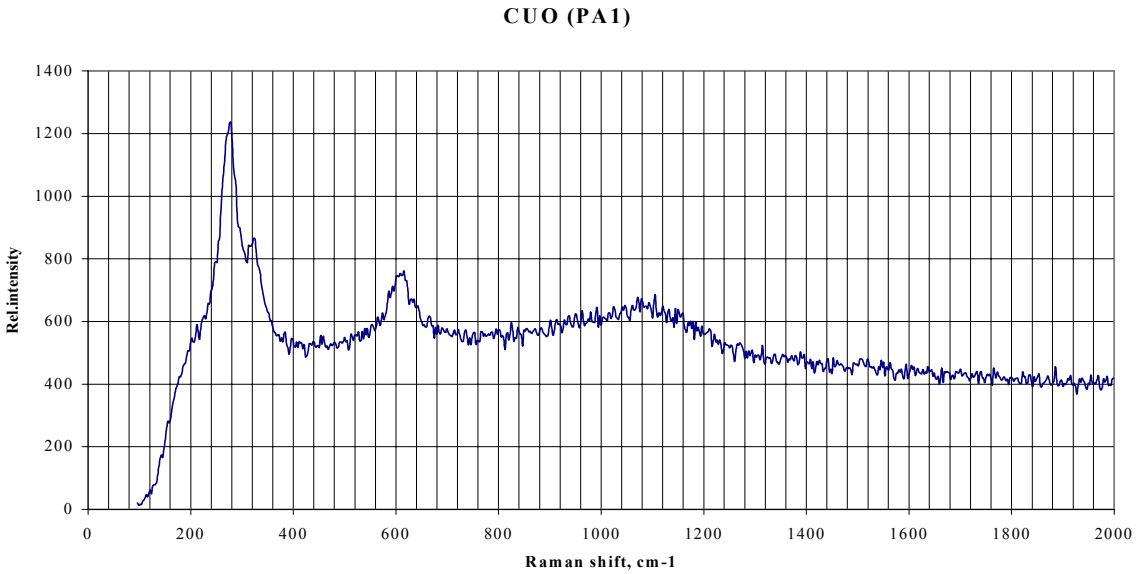

Figure B8
Reference spectrum of CuO.